

Measurements of time-dependent CP violation in $B^0 \rightarrow \psi(2S)K_S^0$ decays

K. Abe,¹⁰ I. Adachi,¹⁰ H. Aihara,⁵² K. Arinstein,¹ T. Aso,⁵⁶ V. Aulchenko,¹ T. Aushev,^{22,16}
 T. Aziz,⁴⁸ S. Bahinipati,³ A. M. Bakich,⁴⁷ V. Balagura,¹⁶ Y. Ban,³⁸ S. Banerjee,⁴⁸
 E. Barberio,²⁵ A. Bay,²² I. Bedny,¹ K. Belous,¹⁵ V. Bhardwaj,³⁷ U. Bitenc,¹⁷ S. Blyth,²⁹
 A. Bondar,¹ A. Bozek,³¹ M. Bračko,^{24,17} J. Brodzicka,¹⁰ T. E. Browder,⁹ M.-C. Chang,⁴
 P. Chang,³⁰ Y. Chao,³⁰ A. Chen,²⁸ K.-F. Chen,³⁰ W. T. Chen,²⁸ B. G. Cheon,⁸
 C.-C. Chiang,³⁰ R. Chistov,¹⁶ I.-S. Cho,⁵⁸ S.-K. Choi,⁷ Y. Choi,⁴⁶ Y. K. Choi,⁴⁶ S. Cole,⁴⁷
 J. Dalseno,²⁵ M. Danilov,¹⁶ A. Das,⁴⁸ M. Dash,⁵⁷ J. Dragic,¹⁰ A. Drutskoy,³ S. Eidelman,¹
 D. Epifanov,¹ S. Fratina,¹⁷ H. Fujii,¹⁰ M. Fujikawa,²⁷ N. Gabyshev,¹ A. Garmash,⁴⁰
 A. Go,²⁸ G. Gokhroo,⁴⁸ P. Goldenzweig,³ B. Golob,^{23,17} M. Grosse Perdekamp,^{12,41}
 H. Guler,⁹ H. Ha,¹⁹ J. Haba,¹⁰ K. Hara,²⁶ T. Hara,³⁶ Y. Hasegawa,⁴⁵ N. C. Hastings,⁵²
 K. Hayasaka,²⁶ H. Hayashii,²⁷ M. Hazumi,¹⁰ D. Heffernan,³⁶ T. Higuchi,¹⁰ L. Hinz,²²
 H. Hoedlmoser,⁹ T. Hokuue,²⁶ Y. Horii,⁵¹ Y. Hoshi,⁵⁰ K. Hoshina,⁵⁵ S. Hou,²⁸
 W.-S. Hou,³⁰ Y. B. Hsiung,³⁰ H. J. Hyun,²¹ Y. Igarashi,¹⁰ T. Iijima,²⁶ K. Ikado,²⁶
 K. Inami,²⁶ A. Ishikawa,⁴² H. Ishino,⁵³ R. Itoh,¹⁰ M. Iwabuchi,⁶ M. Iwasaki,⁵² Y. Iwasaki,¹⁰
 C. Jacoby,²² N. J. Joshi,⁴⁸ M. Kaga,²⁶ D. H. Kah,²¹ H. Kaji,²⁶ S. Kajiwara,³⁶
 H. Kakuno,⁵² J. H. Kang,⁵⁸ P. Kapusta,³¹ S. U. Kataoka,²⁷ N. Katayama,¹⁰ H. Kawai,²
 T. Kawasaki,³³ A. Kibayashi,¹⁰ H. Kichimi,¹⁰ H. J. Kim,²¹ H. O. Kim,⁴⁶ J. H. Kim,⁴⁶
 S. K. Kim,⁴⁴ Y. J. Kim,⁶ K. Kinoshita,³ S. Korpar,^{24,17} Y. Kozakai,²⁶ P. Križan,^{23,17}
 P. Krokovny,¹⁰ R. Kumar,³⁷ E. Kurihara,² A. Kusaka,⁵² A. Kuzmin,¹ Y.-J. Kwon,⁵⁸
 J. S. Lange,⁵ G. Leder,¹⁴ J. Lee,⁴⁴ J. S. Lee,⁴⁶ M. J. Lee,⁴⁴ S. E. Lee,⁴⁴ T. Lesiak,³¹
 J. Li,⁹ A. Limosani,²⁵ S.-W. Lin,³⁰ Y. Liu,⁶ D. Liventsev,¹⁶ J. MacNaughton,¹⁰
 G. Majumder,⁴⁸ F. Mandl,¹⁴ D. Marlow,⁴⁰ T. Matsumura,²⁶ A. Matyja,³¹ S. McOnie,⁴⁷
 T. Medvedeva,¹⁶ Y. Mikami,⁵¹ W. Mitaroff,¹⁴ K. Miyabayashi,²⁷ H. Miyake,³⁶ H. Miyata,³³
 Y. Miyazaki,²⁶ R. Mizuk,¹⁶ G. R. Moloney,²⁵ T. Mori,²⁶ J. Mueller,³⁹ A. Murakami,⁴²
 T. Nagamine,⁵¹ Y. Nagasaka,¹¹ Y. Nakahama,⁵² I. Nakamura,¹⁰ E. Nakano,³⁵ M. Nakao,¹⁰
 H. Nakayama,⁵² H. Nakazawa,²⁸ Z. Natkaniec,³¹ K. Neichi,⁵⁰ S. Nishida,¹⁰ K. Nishimura,⁹
 Y. Nishio,²⁶ I. Nishizawa,⁵⁴ O. Nitoh,⁵⁵ S. Noguchi,²⁷ T. Nozaki,¹⁰ A. Ogawa,⁴¹
 S. Ogawa,⁴⁹ T. Ohshima,²⁶ S. Okuno,¹⁸ S. L. Olsen,⁹ S. Ono,⁵³ W. Ostrowicz,³¹
 H. Ozaki,¹⁰ P. Pakhlov,¹⁶ G. Pakhlova,¹⁶ H. Palka,³¹ C. W. Park,⁴⁶ H. Park,²¹
 K. S. Park,⁴⁶ N. Parslow,⁴⁷ L. S. Peak,⁴⁷ M. Pernicka,¹⁴ R. Pestotnik,¹⁷ M. Peters,⁹
 L. E. Pilonen,⁵⁷ A. Poluektov,¹ J. Rorie,⁹ M. Rozanska,³¹ H. Sahoo,⁹ Y. Sakai,¹⁰
 H. Sakamoto,²⁰ H. Sakaue,³⁵ T. R. Sarangi,⁶ N. Satoyama,⁴⁵ K. Sayeed,³ T. Schietinger,²²
 O. Schneider,²² P. Schönmeier,⁵¹ J. Schümann,¹⁰ C. Schwanda,¹⁴ A. J. Schwartz,³
 R. Seidl,^{12,41} A. Sekiya,²⁷ K. Senyo,²⁶ M. E. Sevier,²⁵ L. Shang,¹³ M. Shapkin,¹⁵
 C. P. Shen,¹³ H. Shibuya,⁴⁹ S. Shinomiya,³⁶ J.-G. Shiu,³⁰ B. Shwartz,¹ J. B. Singh,³⁷
 A. Sokolov,¹⁵ E. Solovieva,¹⁶ A. Somov,³ S. Stanič,³⁴ M. Starič,¹⁷ J. Stypula,³¹
 A. Sugiyama,⁴² K. Sumisawa,¹⁰ T. Sumiyoshi,⁵⁴ S. Suzuki,⁴² S. Y. Suzuki,¹⁰ O. Tajima,¹⁰
 F. Takasaki,¹⁰ K. Tamai,¹⁰ N. Tamura,³³ M. Tanaka,¹⁰ N. Taniguchi,²⁰ G. N. Taylor,²⁵
 Y. Teramoto,³⁵ I. Tikhomirov,¹⁶ K. Trabelsi,¹⁰ Y. F. Tse,²⁵ T. Tsuboyama,¹⁰ K. Uchida,⁹

arXiv:0708.2604v1 [hep-ex] 20 Aug 2007

Y. Uchida,⁶ S. Uehara,¹⁰ K. Ueno,³⁰ T. Uglov,¹⁶ Y. Unno,⁸ S. Uno,¹⁰ P. Urquijo,²⁵
Y. Ushiroda,¹⁰ Y. Usov,¹ G. Varner,⁹ K. E. Varvell,⁴⁷ K. Vervink,²² S. Villa,²²
A. Vinokurova,¹ C. C. Wang,³⁰ C. H. Wang,²⁹ J. Wang,³⁸ M.-Z. Wang,³⁰ P. Wang,¹³
X. L. Wang,¹³ M. Watanabe,³³ Y. Watanabe,¹⁸ R. Wedd,²⁵ J. Wicht,²² L. Widhalm,¹⁴
J. Wiechczynski,³¹ E. Won,¹⁹ B. D. Yabsley,⁴⁷ A. Yamaguchi,⁵¹ H. Yamamoto,⁵¹
M. Yamaoka,²⁶ Y. Yamashita,³² M. Yamauchi,¹⁰ C. Z. Yuan,¹³ Y. Yusa,⁵⁷ C. C. Zhang,¹³
L. M. Zhang,⁴³ Z. P. Zhang,⁴³ V. Zhilich,¹ V. Zhulanov,¹ A. Zupanc,¹⁷ and N. Zwahlen²²

(The Belle Collaboration)

¹*Budker Institute of Nuclear Physics, Novosibirsk*

²*Chiba University, Chiba*

³*University of Cincinnati, Cincinnati, Ohio 45221*

⁴*Department of Physics, Fu Jen Catholic University, Taipei*

⁵*Justus-Liebig-Universität Gießen, Gießen*

⁶*The Graduate University for Advanced Studies, Hayama*

⁷*Gyeongsang National University, Chinju*

⁸*Hanyang University, Seoul*

⁹*University of Hawaii, Honolulu, Hawaii 96822*

¹⁰*High Energy Accelerator Research Organization (KEK), Tsukuba*

¹¹*Hiroshima Institute of Technology, Hiroshima*

¹²*University of Illinois at Urbana-Champaign, Urbana, Illinois 61801*

¹³*Institute of High Energy Physics,*

Chinese Academy of Sciences, Beijing

¹⁴*Institute of High Energy Physics, Vienna*

¹⁵*Institute of High Energy Physics, Protvino*

¹⁶*Institute for Theoretical and Experimental Physics, Moscow*

¹⁷*J. Stefan Institute, Ljubljana*

¹⁸*Kanagawa University, Yokohama*

¹⁹*Korea University, Seoul*

²⁰*Kyoto University, Kyoto*

²¹*Kyungpook National University, Taegu*

²²*Ecole Polytechnique Fédérale Lausanne, EPFL, Lausanne*

²³*University of Ljubljana, Ljubljana*

²⁴*University of Maribor, Maribor*

²⁵*University of Melbourne, School of Physics, Victoria 3010*

²⁶*Nagoya University, Nagoya*

²⁷*Nara Women's University, Nara*

²⁸*National Central University, Chung-li*

²⁹*National United University, Miao Li*

³⁰*Department of Physics, National Taiwan University, Taipei*

³¹*H. Niewodniczanski Institute of Nuclear Physics, Krakow*

³²*Nippon Dental University, Niigata*

³³*Niigata University, Niigata*

³⁴*University of Nova Gorica, Nova Gorica*

³⁵*Osaka City University, Osaka*

³⁶*Osaka University, Osaka*

³⁷*Panjab University, Chandigarh*

- ³⁸*Peking University, Beijing*
³⁹*University of Pittsburgh, Pittsburgh, Pennsylvania 15260*
⁴⁰*Princeton University, Princeton, New Jersey 08544*
⁴¹*RIKEN BNL Research Center, Upton, New York 11973*
⁴²*Saga University, Saga*
⁴³*University of Science and Technology of China, Hefei*
⁴⁴*Seoul National University, Seoul*
⁴⁵*Shinshu University, Nagano*
⁴⁶*Sungkyunkwan University, Suwon*
⁴⁷*University of Sydney, Sydney, New South Wales*
⁴⁸*Tata Institute of Fundamental Research, Mumbai*
⁴⁹*Toho University, Funabashi*
⁵⁰*Tohoku Gakuin University, Tagajo*
⁵¹*Tohoku University, Sendai*
⁵²*Department of Physics, University of Tokyo, Tokyo*
⁵³*Tokyo Institute of Technology, Tokyo*
⁵⁴*Tokyo Metropolitan University, Tokyo*
⁵⁵*Tokyo University of Agriculture and Technology, Tokyo*
⁵⁶*Toyama National College of Maritime Technology, Toyama*
⁵⁷*Virginia Polytechnic Institute and State University, Blacksburg, Virginia 24061*
⁵⁸*Yonsei University, Seoul*

Abstract

We report improved measurements of time-dependent CP violation parameters for $B^0(\overline{B}^0) \rightarrow \psi(2S)K_S^0$. This analysis is based on a data sample of 657×10^6 $B\overline{B}$ pairs collected at the $\Upsilon(4S)$ resonance with the Belle detector at the KEKB energy-asymmetric e^+e^- collider. CP violation parameters are obtained from the asymmetries in the distributions of the proper-time intervals between the two B decays

$$\mathcal{S}_{\psi(2S)K_S^0} = +0.72 \pm 0.09(\text{stat}) \pm 0.03(\text{syst})$$

$$\mathcal{A}_{\psi(2S)K_S^0} = +0.04 \pm 0.07(\text{stat}) \pm 0.05(\text{syst})$$

and are in agreement with results from measurements of $B^0 \rightarrow J/\psi K^0$.

PACS numbers:

In the Standard Model (SM), CP violation in B^0 meson decays originates from an irreducible complex phase in the 3×3 Cabibbo-Kobayashi-Maskawa (CKM) mixing matrix [1]. In the decay chain $\Upsilon(4S) \rightarrow B^0 \bar{B}^0 \rightarrow f_{CP} f_{\text{tag}}$, where one of the B mesons decays at time t_{CP} to a CP eigenstate f_{CP} and the other decays at time t_{tag} to a final state f_{tag} that distinguishes between B^0 and \bar{B}^0 , the decay rate has a time dependence [2] given by

$$\mathcal{P}(\Delta t) = \frac{e^{-|\Delta t|/\tau_{B^0}}}{4\tau_{B^0}} \left\{ 1 + q \cdot \left[\mathcal{S}_{f_{CP}} \sin(\Delta m_d \Delta t) + \mathcal{A}_{f_{CP}} \cos(\Delta m_d \Delta t) \right] \right\}. \quad (1)$$

Here $\mathcal{S}_{f_{CP}}$ and $\mathcal{A}_{f_{CP}}$ are the CP violation parameters, τ_{B^0} is the B^0 lifetime, Δm_d is the mass difference between the two B^0 mass eigenstates, $\Delta t = t_{CP} - t_{\text{tag}}$, and the b -flavor charge q equals $+1$ (-1) when the tagging B meson is a B^0 (\bar{B}^0). For decays that proceed via the transition $b \rightarrow c\bar{c}s$, the SM predicts $\mathcal{S}_{f_{CP}} = -\xi_f \sin 2\phi_1$ and $\mathcal{A}_{f_{CP}} \simeq 0$, where $\xi_f = +1$ (-1) for CP -even (CP -odd) final states. Previous measurements of CP asymmetries in $b \rightarrow c\bar{c}s$ transitions have been reported by Belle [3, 4] and BaBar [5]. Results from our previously published $B^0 \rightarrow \psi(2S)K_S^0$ analysis was based on a 140 fb^{-1} data sample corresponding to 152×10^6 $B\bar{B}$ pairs [3]. Here we report new measurements incorporating an additional 465 fb^{-1} data sample for a total of 605 fb^{-1} (657×10^6 $B\bar{B}$ pairs).

At the KEKB energy-asymmetric e^+e^- (3.5 on 8.0 GeV) collider [6], the $\Upsilon(4S)$ is produced with a Lorentz boost of $\beta\gamma = 0.425$ nearly along the z axis, which is defined as opposite to the positron beam direction. Since the B^0 and \bar{B}^0 are approximately at rest in the $\Upsilon(4S)$ center-of-mass system (cms), Δt can be determined from the displacement in z between the two decay vertices: $\Delta t \simeq \Delta z/(\beta\gamma c)$.

The Belle detector is a large-solid-angle magnetic spectrometer that consists of a silicon vertex detector (SVD), a 50-layer central drift chamber (CDC), an array of aerogel threshold Čerenkov counters (ACC), a barrel-like arrangement of time-of-flight scintillation counters (TOF), and an electromagnetic calorimeter (ECL) comprised of CsI(Tl) crystals located inside a superconducting solenoid coil that provides a 1.5 T magnetic field. An iron flux-return located outside the coil is instrumented to detect K_L^0 mesons and to identify muons (KLM). The detector is described in detail elsewhere [7]. Two different inner detector configurations were used. For the first sample of 152×10^6 $B\bar{B}$ pairs, a 2.0 cm radius beampipe and a 3-layer silicon vertex detector (SVD-I) were used; for the latter 505×10^6 $B\bar{B}$ pairs, a 1.5 cm radius beampipe, a 4-layer silicon detector (SVD-II), and a small-cell inner drift chamber were used [8].

We reconstruct $\psi(2S)$ mesons in the l^+l^- decay channel ($l = e$ or μ) and $J/\psi\pi^+\pi^-$ decay channel. J/ψ mesons are reconstructed in the l^+l^- decay channel and include up to two Bremsstrahlung photons that are within 50 mrad of each of the e^+ and e^- tracks (denoted as $e^+e^-(\gamma)$). The invariant mass of the J/ψ candidates is required to be within $-0.150 \text{ GeV}/c^2 < M_{e^+e^-(\gamma)} - m_{J/\psi} < +0.036 \text{ GeV}/c^2$ and $-0.060 \text{ GeV}/c^2 < M_{\mu^+\mu^-} - m_{J/\psi} < +0.036 \text{ GeV}/c^2$, where $m_{J/\psi}$ denotes the J/ψ nominal mass, and $M_{e^+e^-(\gamma)}$ and $M_{\mu^+\mu^-}$ are the reconstructed invariant masses of $e^+e^-(\gamma)$ and $\mu^+\mu^-$ respectively. For the $\psi(2S) \rightarrow l^+l^-$ candidates, the invariant mass is required to be within $-0.150 \text{ GeV}/c^2 < M_{e^+e^-(\gamma)} - m_{\psi(2S)} < +0.036 \text{ GeV}/c^2$ and $-0.060 \text{ GeV}/c^2 < M_{\mu^+\mu^-} - m_{\psi(2S)} < +0.036 \text{ GeV}/c^2$, where $m_{\psi(2S)}$ denotes the $\psi(2S)$ nominal mass. For the $\psi(2S) \rightarrow J/\psi\pi^+\pi^-$ candidates, $\Delta M = M_{l^+l^-\pi^+\pi^-} - M_{l^+l^-}$ is required to be within $0.580 \text{ GeV}/c^2 < \Delta M < 0.600 \text{ GeV}/c^2$. To reduce the incorrectly reconstructed signal candidates, we select $\pi^+\pi^-$ pairs with an invariant mass greater than $400 \text{ MeV}/c^2$ [3]. The K_S^0 selection criteria are the same as those described in Ref. [9], the invariant mass of the pion pairs is required to be within $0.482 \text{ GeV}/c^2 < M_{\pi^+\pi^-} < 0.514 \text{ GeV}/c^2$.

We combine the $\psi(2S)$ and K_S^0 to form a neutral B meson. Signal candidates are identified using the energy difference $\Delta E \equiv E_B^{\text{cms}} - E_{\text{beam}}^{\text{cms}}$ and the beam-energy-constrained mass $M_{\text{bc}} \equiv \sqrt{(E_{\text{beam}}^{\text{cms}})^2 - (p_B^{\text{cms}})^2}$, where $E_{\text{beam}}^{\text{cms}}$ is the beam energy in the cms, and E_B^{cms} and p_B^{cms} are the cms energy and momentum, respectively, of the reconstructed B candidate. The signal candidates are selected by requiring $5.27 \text{ GeV}/c^2 < M_{\text{bc}} < 5.29 \text{ GeV}/c^2$ and $|\Delta E| < 0.030 \text{ GeV}$.

The b -flavor of the accompanying B meson is identified by a tagging algorithm [10] that categorizes charged leptons, kaons and Λ baryons found in the event. The algorithm returns two parameters: the b -flavor charge q and r , which indicates the tag quality as determined from MC simulation and varies from $r = 0$ for no flavor discrimination to $r = 1$ for unambiguous flavor assignment. If $r < 0.1$, the accompanying B meson provides negligible tagging information and we set the wrong tag probability to 0.5. Events with $r > 0.1$ are sorted into six intervals.

The vertex position for the f_{CP} decay is reconstructed using charged tracks that have enough SVD hits [11]. A constraint on the interaction point (IP) is also used with the selected tracks; the IP profile is convolved with the finite B -flight length in the plane perpendicular to the z axis. The pions from K_S^0 decays are not used for vertexing. The typical vertex reconstruction efficiency and z resolution are 95% and $78 \mu\text{m}$, respectively. The f_{tag} vertex determination is obtained with well-reconstructed tracks that are not assigned to f_{CP} . The typical vertex reconstruction efficiency and z resolution are 93% and $140 \mu\text{m}$, respectively. After all selection criteria are applied, we obtain 1617 and 1202 events for the l^+l^- and $J/\psi\pi^+\pi^-$ modes in the $\Delta E - M_{\text{bc}}$ fit region defined as $5.2 \text{ GeV}/c^2 < M_{\text{bc}} < 5.3 \text{ GeV}/c^2$ and $-0.1 \text{ GeV} < \Delta E < 0.1 \text{ GeV}$, of which 680 and 712 are in the signal box.

Figure 1 shows the reconstructed variables M_{bc} and ΔE after flavor tagging and vertex reconstruction. The signal yield is obtained from an unbinned maximum-likelihood fit to these distributions. The signal shape for each decay mode is determined from Monte Carlo (MC) events; these shapes are adjusted for small differences between MC and data using a control sample of $B^- \rightarrow \psi(2S)K^-$ events, which have a final state similar to the signal but with higher statistics. This sample, where no CP asymmetry is expected, will be also used to check the potential bias in the CP violation parameter measurements. The signal yields in the ΔE - M_{bc} signal window are 628 and 656; the purity is 94% in both modes (Table I).

TABLE I: Number of signal B candidates after flavor tagging and vertex reconstruction, N_{sig} , and the estimated signal purity, p .

Mode	N_{sig}	p (%)
$\psi(2S)(l^+l^-)K_S^0$	628 ± 26	94.1 ± 0.4
$\psi(2S)(J/\psi\pi^+\pi^-)K_S^0$	656 ± 26	94.1 ± 0.4

In the signal probability density function (PDF) (Eq. 1), the effect of incorrect flavor assignment is incorporated and the result is convolved with a resolution function $R_{\text{sig}}(\Delta t)$ to take into account the finite vertex resolution. The resolution function parameters, along with the wrong tag fractions for the six r intervals, w_l ($l = 1, 6$) and possible differences in w_l between B^0 and \bar{B}^0 decays (Δw_l) are determined using a high-statistics control sample of semileptonic and hadronic $b \rightarrow c$ decays [3].

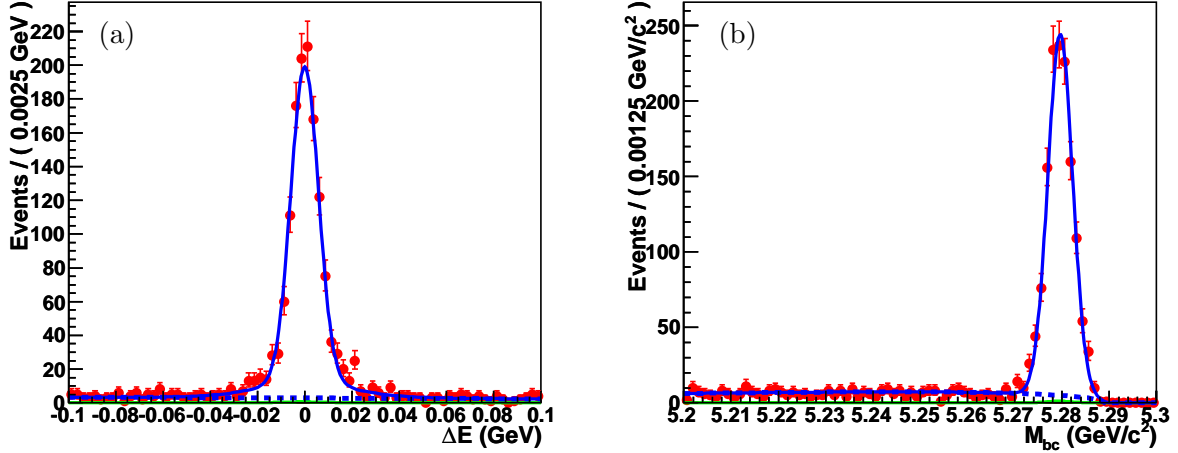


FIG. 1: (a) ΔE distribution within the M_{bc} signal region, (b) M_{bc} distribution within the ΔE signal region for $B^0 \rightarrow \psi(2S)K_S^0$. The solid curves show the fits to signal plus background distributions, while the dashed curves show the background contributions. The small contribution from peaking backgrounds is discussed in the text.

We determine the following likelihood for each event:

$$\begin{aligned}
 P_i = & (1 - f_{ol}) \int \left[f_{sig} \mathcal{P}_{sig}(\Delta t') R_{sig}(\Delta t_i - \Delta t') + f_{peak} \mathcal{P}_{peak}(\Delta t') R_{sig}(\Delta t_i - \Delta t') \right. \\
 & \left. + (1 - f_{sig} - f_{peak}) \mathcal{P}_{bkg}(\Delta t') R_{bkg}(\Delta t_i - \Delta t') \right] d(\Delta t') + f_{ol} P_{ol}(\Delta t_i). \quad (2)
 \end{aligned}$$

The signal probability f_{sig} depends on the r region and is calculated on an event-by-event basis as a function of M_{bc} and ΔE .

In Eq. 2, the PDF for background events, $\mathcal{P}_{bkg}(\Delta t)$, is modeled as a sum of exponential and prompt components and is convolved with a sum of two Gaussians, R_{bkg} . Parameters in $\mathcal{P}_{bkg}(\Delta t)$ and R_{bkg} are determined from a fit to the Δt distribution for events in a ΔE - M_{bc} data sideband ($M_{bc} < 5.26 \text{ GeV}/c^2$, $-0.03 \text{ GeV} < \Delta E < 0.20 \text{ GeV}$). For $\psi(2S) \rightarrow J/\psi \pi^+ \pi^-$ mode, a background component that peaks like the signal in ΔE - M_{bc} (peaking background) is added. This peaking background is mainly due to $J/\psi K_1^0(1270)$, $J/\psi K^{*-}(892)\pi^+$ and $J/\psi K_S^0 \pi^+ \pi^-$ modes, with no real $\psi(2S) \rightarrow J/\psi \pi^+ \pi^-$ in the final state. The fraction of such events is estimated directly from the sideband of ΔM distribution in data (1%). The corresponding PDF, $\mathcal{P}_{peak}(\Delta t)$, is the same as $\mathcal{P}_{sig}(\Delta t)$ with CP parameters fixed to zero. The term $P_{ol}(\Delta t)$ is a broad Gaussian function that represents an outlier component with a small fraction f_{ol} . The only free parameters in the final fit are $\mathcal{S}_{f_{CP}}$ and $\mathcal{A}_{f_{CP}}$; these are determined by maximizing the likelihood function $L = \prod_i P_i(\Delta t_i; \mathcal{S}_{f_{CP}}, \mathcal{A}_{f_{CP}})$ where the product is over all events.

The unbinned maximum likelihood fit to the 1392 events in the signal region results in the CP violation parameters:

$$\mathcal{S}_{\psi(2S)K_S^0} = +0.72 \pm 0.09(\text{stat}) \pm 0.03(\text{syst})$$

$$\mathcal{A}_{\psi(2S)K_S^0} = +0.04 \pm 0.07(\text{stat}) \pm 0.05(\text{syst}),$$

where the systematic uncertainties listed are described below. We define the raw asymmetry in each Δt bin by $(N_+ - N_-)/(N_+ + N_-)$, where $N_{+(-)}$ is the number of observed candidates with $q = +1$ (-1). Figure 2 shows this asymmetry for events with good tagging quality ($r > 0.5$).

The dominant sources of systematic error for $\mathcal{S}_{f_{CP}}$ are the uncertainties in the vertex reconstruction (0.026), in the fit bias (0.012) and in the resolution function (0.007). The dominant sources of systematic error for $\mathcal{A}_{f_{CP}}$ are the effects of tag-side interference [12] (0.036), the uncertainties in the vertex reconstruction (0.020). Other contributions come from uncertainties in wrong tag fractions, lifetime and mixing. A possible fit bias is examined by fitting a large number of MC events. We add each contribution above in quadrature to obtain the total systematic uncertainty. The systematic uncertainties are summarized in Table II.

TABLE II: Systematic uncertainties.

Parameter	$\Delta\mathcal{S}_{\psi(2S)K_S^0}$	$\Delta\mathcal{A}_{\psi(2S)K_S^0}$
Vertexing	0.026	0.020
Wrong tag fraction	0.006	0.023
Resolution function	0.007	0.005
Fit bias	0.012	0.011
Physics parameters	0.001	0.001
Peaking background	0.006	0.005
PDF shape and fraction	0.001	0.003
Background Δt shape	0.003	0.003
Tag side interference	0.011	0.036
Total	0.033	0.049

In summary, we have performed improved measurements of CP violation parameters $\sin 2\phi_1$ and $\mathcal{A}_{f_{CP}}$ for $B^0 \rightarrow \psi(2S)K_S^0$ using 657×10^6 $B\bar{B}$ events. These measurements supersede our previous result [3] and are in agreement with results from measurements of $B^0 \rightarrow J/\psi K^0$ [13].

Acknowledgments

We thank the KEKB group for the excellent operation of the accelerator, the KEK cryogenics group for the efficient operation of the solenoid, and the KEK computer group and the National Institute of Informatics for valuable computing and Super-SINET network support. We acknowledge support from the Ministry of Education, Culture, Sports, Science, and Technology of Japan and the Japan Society for the Promotion of Science; the Australian Research Council and the Australian Department of Education, Science and Training; the National Science Foundation of China and the Knowledge Innovation Program of the Chinese Academy of Sciences under contract No. 10575109 and IHEP-U-503; the Department of

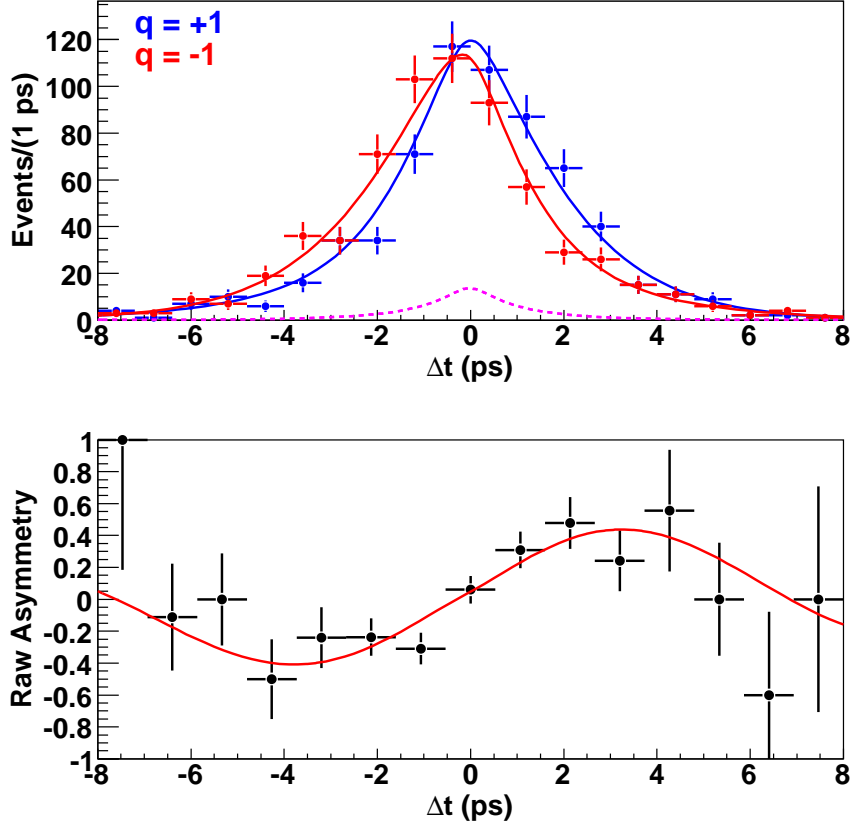


FIG. 2: Δt distributions of $B^0 \rightarrow \psi(2S)K_S^0$ for $q = +1$ and $q = -1$. The dashed line is the sum of backgrounds while the solid lines are the sum of signal and backgrounds. The bottom plot is the raw asymmetry of well-tagged events ($r > 0.5$). The solid curve shows the result of the unbinned maximum-likelihood fit.

Science and Technology of India; the BK21 program of the Ministry of Education of Korea, the CHEP SRC program and Basic Research program (grant No. R01-2005-000-10089-0) of the Korea Science and Engineering Foundation, and the Pure Basic Research Group program of the Korea Research Foundation; the Polish State Committee for Scientific Research; the Ministry of Education and Science of the Russian Federation and the Russian Federal Agency for Atomic Energy; the Slovenian Research Agency; the Swiss National Science Foundation; the National Science Council and the Ministry of Education of Taiwan; and the U.S. Department of Energy.

-
- [1] N. Cabbibo, Phys. Rev. Lett. **10**, 531 (1963); M. Kobayashi and T. Maskawa, Prog. Theor. Phys. **49**, 652 (1973).
[2] A. B. Carter and A. I. Sanda, Phys. Rev. D **23**, 1567 (1981); I. I. Bigi and A. I. Sanda, Nucl. Phys. B **193**, 85 (1981).
[3] K. Abe *et al.* (Belle Collaboration), Phys. Rev. D **71**, 072003 (2005).

- [4] K-F. Chen *et al.* (Belle Collaboration), Phys. Rev. Lett. **98**, 031802 (2007).
- [5] B. Aubert *et al.* (BaBar Collaboration), hep-ex/0703021 (submitted to Phys. Rev. Lett.).
- [6] S. Kurokawa and E. Kikutani, Nucl. Instrum. Methods Phys. Res., Sect. A **499**, 1 (2003), and other papers included in this volume.
- [7] A. Abashian *et al.* (Belle Collaboration), Nucl. Instr. and Meth. A **479**, 117 (2002).
- [8] Z. Natkaniec (Belle SVD2 Group), Nucl. Instr. and Meth.A **560**, 1 (2006).
- [9] K-F. Chen *et al.* (Belle Collaboration), Phys. Rev. D **72**, 012004 (2005).
- [10] H. Kakuno *et al.*, Nucl. Instr. and Meth.A **533**, 516 (2004).
- [11] H. Tajima *et al.*, Nucl. Instrum. Methods Phys. Res., Sect. A **533**, 370 (2004).
- [12] O. Long, M. Baak, R. N. Cahn and D. Kirkby, Phys. Rev. D **68**, 034010 (2003).
- [13] Heavy Flavour Averaging Group, E. Barberio *et al.*, hep-ex/0603003. See <http://www.slac.stanford.edu/xorg/hfag/> for updated results.